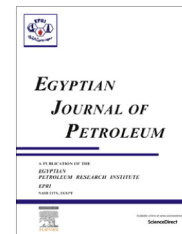


HOSTED BY



Egyptian Petroleum Research Institute
Egyptian Journal of Petroleum

www.elsevier.com/locate/egyjp
www.sciencedirect.com



FULL LENGTH ARTICLE

Enhancement of yield point at high pressure high temperature wells by using polymer nanocomposites based on ZnO & CaCO₃ nanoparticles

A.Z. Noah^{a,*}, M.A. El Semary^b, A.M. Youssef^c, M.A. El-Safty^d

^a Materials Department, National Research Centre, 33 El Bohouth St. (former El Tahrir st.), P.O. 12622, Dokki, Giza, Egypt

^b Misr Petroleum Company, Alexandria, Egypt

^c Packing and Packaging Materials Department, National Research Centre, Egypt

^d Faculty of science, Zagazig University, Cairo, Egypt

Received 6 December 2015; revised 15 February 2016; accepted 6 March 2016

KEYWORDS

Nanocomposites;
 ZnO-NPs;
 Nano-CaCO₃;
 HPHT;
 Oil base mud;
 Drilling fluid

Abstract Zinc oxide nanoparticles (ZnO-NPs) and modified calcium carbonate (nano-CaCO₃) nanoparticles were successfully prepared and added to polystyrene-butadiene rubber copolymer (PSBR) matrix to prepare PSBR nanocomposites. The prepared nanomaterials (ZnO-NPs & nano-CaCO₃) were characterized using scanning electron microscope (SEM), transmission electron microscope (TEM) and X-ray diffraction (XRD). Furthermore, the prepared polymer nanocomposites and oil base mud were used for drilling in high pressure high temperature (HPHT) wells. The consequence of using polymer nanocomposites based on different loading of ZnO-NPs and nano-CaCO₃ on the rheological properties of oil base mud was evaluated and enhanced the yield point at high pressure high temperature wells (HPHT). The using of the polymer with different percentage from (0.5) in all percent the obtained results is very promising; this means that the increase of polymer is reasonable for the increase of apparent viscosity, plastic viscosity and yield point at high temperature. Correspondingly, polymer nanocomposites displayed rise of apparent viscosity, plastic viscosity, and yield point, decreased in fluid loss and increased in electrical stability at high pressure high temperature wells.

© 2016 Egyptian Petroleum Research Institute. Production and hosting by Elsevier B.V. This is an open access article under the CC BY-NC-ND license (<http://creativecommons.org/licenses/by-nc-nd/4.0/>).

1. Introduction

The exploration and production of oil and gas is falling into deepwater reservoirs in HPHT environments. Consequently,

* Corresponding author.

E-mail address: alaanooh@hotmail.com (A.Z. Noah).

Peer review under responsibility of Egyptian Petroleum Research Institute.

<http://dx.doi.org/10.1016/j.ejpe.2016.03.002>

1110-0621 © 2016 Egyptian Petroleum Research Institute. Production and hosting by Elsevier B.V.

This is an open access article under the CC BY-NC-ND license (<http://creativecommons.org/licenses/by-nc-nd/4.0/>).

HPHT wells are becoming very motivating. The inherent conditions of these wells cause the rheological parameters of fluids to differ enormously. Challenges of HPHT wells include the high cost essential for the equipment and the materials that are able to standing these extreme pressures and temperatures. The narrow boundary between the pore pressure and fracture gradient is also significant challenge that should be extremely considered. Additionally, HPHT wells frequently have high ECD leading to down hole problems such as mud losses into

the formation. We, therefore, are constantly looking for new methods and solutions to ensure high cleaning efficiency and overcome the hazards of these over pressured formations.

The cost reduction may be accomplished generally by three ways, increasing the drilling productivity by minimizing well bore instabilities, lowering the cost of fluids and avoiding modification, and over engineering of the fluid and reducing the number of platform and wells [1,2]. The configuration of drilling mud will depend on the requirements of the specific drilling operation. Holes must be drilled through different kinds of formation, requiring different types of drilling fluid. Economics, contamination, obtainable make up water, pressure and temperature are main factor in drilling fluid process [3].

Water alone is occasionally an ideal drilling fluid and normally used to drill areas where trouble free low pressure formation occurs. In some areas, drilling can be started with water and the drilled solid combined into the water resultant in a sensibly good mud. In other areas, it may be essential to add commercial clays to the water prior for starting drilling operation, the clay serves as dual purpose: first, to give viscosity to the drilling fluid and second, to seal the walls of the hole that the fluid circulated will not be lost to permeable formation being drilled.

There are various mud additives that are called “polymers and polymer nanocomposites”. A strict definition of a polymer is an organic chemical having a molecular weight above 200, with greater than eight repeating units. They vary significantly in function and basic properties, i.e., stability, charge. In general, polymers can be classified as natural, modified-natural and synthetic [4]. Many types of polymer can be supplementary to clear water to support in the flocculation and settling of drilled solids at the surface. When used properly, these polymers used with an electrolyte for example lime or calcium chloride can keep drilling water clean and clear at the suction. Polyacrylates are synthetic materials from petroleum feedstocks [5]. They are not as difficult structurally as the natural polymers and usually have a straight-chain carbon backbone with different side chains, depending on the desired end product. They are usually anionic for examples: polyacrylates, copolymers, vinyl acetate, vinyl polymers, and maleic anhydride. Their uses are: low molecular weight (<1000)-thinners and deflocculates; medium molecular weight (up to 100,000 MW) – fluid loss control, flocculants and shale stabilizers; high molecular weight (> 100,000 MW) bentonite extenders and flocculants. Nanocomposites based on polymeric matrices gained significant importance after the report of nanoclays filled nylon-6 by [6], but the real mention of the term was first found in the work of [7]. Amazingly automobile tires in which carbon black acts as a reinforcement are also an instance of a nanocomposites. However, the term “nanocomposite” is not frequently used to designate such composites. Nanocomposites are considered to be a multiphase solid material where one of the phases has one, two or three dimensions of less than 100 nm according to [8] and this nanocomposites used for different applications [9,10].

In the field of materials in general and of nanocomposites in particular, one of the most commonly used inorganic fillers is calcium carbonate (CaCO_3) because of its low cost, high capacity to be dispersed in a polymeric matrix and its potential to improve the mechanical properties of the polymer compounds [11,12]. Moreover, ZnO is an eco-friendly nanoparticle and has attracted wide attention due to its good antibacterial

properties, high stability, photocatalytic activity and non-toxicity [13]. ZnO-NPs have several important applications in biomedical field [14], as food additive, and in catalysis [15]. The incorporation of ZnO nanoparticles to polymers matrix as nanofillers could improve not only the fabricated nanocomposites, mechanical and barrier properties but also create other functions and applications in food packaging such as antimicrobial agent [16].

2. Experimental details

2.1. Materials

Polystyrene butadiene rubber copolymer (PSBR) was obtained from Misr petroleum Company, Egypt. Zn (CH_3COO)₂·2H₂O (99.5%), zinc acetate dihydrate (99% purity) and sodium hydroxide (pellet .99%) as the introductory material were supplied by Sigma–Aldrich chemicals. Calcium carbonate nanoparticles (nano- CaCO_3) were supplied from Formosa plastics corporation Taipei, Taiwan and used as received. Calcium carbonate nanoparticles with surface coating of stearic acid were purchased from Malaysian Nuclear Agency

2.2. Methods

2.2.1. Preparation of ZnO nanoparticles

In order to prepare zinc oxide nanoparticles (ZnO-NPs) [17], stock solutions of Zn(CH_3COO)₂·2H₂O (0.2 M) were prepared in 50 ml methanol under stirring. To this stock solution 50 ml of NaOH (varying from 0.4 M to 0.8 M) in methanol was added under constant stirring in order to get the pH value of reactants between 8 and 11. These solutions was transferred into Teflon lined sealed stainless steel autoclaves and continuous at various temperature in the range of 100–200 °C for 6 and 12 h under autogenously pressure. It was then allowed to cool naturally to room temperature. After the reaction was complete, the resulting white solid products were washed with methanol, filtered and then dried in a laboratory oven at 60 °C

2.2.2. Modification of CaCO_3 nanoparticles using stearic acid

Appropriate amount of CaCO_3 nanoparticle was added to stirred solution of stearic acid in CH_2Cl_2 . The mixture was stirred 30 min, was then ultrasonically agitated for 30 min, and further stirred for 24 h at 25 °C. The solvent was evaporated in vacuum and the residue was extracted with CH_2Cl_2 using Soxhelt apparatus for another 24 h until no acid was detected in the extract. The solution was then filtered and the precipitate was rinsed thoroughly with a mixture of alcohol and deionized water. The precipitate was kept in a vacuum oven for 24 h at 100 °C. A white powder of modified CaCO_3 nanoparticles was obtained.

2.2.3. Preparation of PSBR/ZnO nanocomposites

For the preparation of PSBR/ZnO nanocomposites, 0.5 g of polystyrene butadiene rubber copolymer (PSBR) was dissolved in 10 ml of toluene to obtain a 5% solution after one hour of stirring. The PSBR/ZnO nanocomposite solution was set by adding ZnO-NPs powder into PSB solution and the mixture was stirred for three hour and then sonicated for five minutes,

and the mixture is thermally aged in hot rolling with oil base mud over for 16 h at 350 °F. After 16 h the mixture is out and the rheological parameters are measured again using the HPHT viscometer at 120 °F (at 500 psi) and the HPHT fluid loss at 350 °F (at 500 psi). This nanocomposite with oil base mud was used for drilling in HPHT wells.

2.2.4. Preparation of PSBR/CaCO₃ nanocomposites

The preparation of PSBR/CaCO₃ nanocomposites, 0.5 g of PSBR was dissolved in 10 ml of toluene to obtain a 5% solution after one hour of stirring. The polymer nanocomposite solution was prepared by adding modified nano-CaCO₃ powder into PSBR solution and the mixture was stirred for 16 h and then sonicated for 30 min, and the mixture is thermally aged in hot rolling with oil base mud over for 16 h at 350 °F. After 16 h the mixture is out and the rheological parameters are measured another time using the HPHT viscometer at 120 °F and the HPHT fluid loss at 350 °F and 500 psi. This nanocomposite with oil base mud was used for drilling in HPHT wells.

2.2.5. Preparation of oil base mud sample at Egyptian Mud Engineering Company (EMEC)

2.2.5.1. Composition of oil base mud sample. This method involves in mixing of the raw materials in different percentages; after this, the freshwater is added to mixture drop by drop through stirrer in barrel for 1 h (Table 1). Then they are put in thermo cup using different temperatures. The next step is to measure the mud rheology by HPHT viscometer. Controlling mud weight depends on the percentage of diesel and barite.

Mud weight of this sample = 12 PPg.

Oil/water ratio = 88/12.

2.3. Characterization

2.3.1. X-ray diffraction (XRD)

The crystal structure of the filler powders was determined using a Philips X-ray diffractometer (PW 1930 generator, PW 1820 goniometer), equipped with Cu K α radiation (45 kV, 40 mA, with $\lambda = 0.15418$ nm). The scans of the analysis were run in 2θ range of 5–80° with step size of 0.02 and step time of 1 s.

2.3.2. Fourier transmission infrared spectroscopy (FT-IR)

FT-IR spectra of nano-CaCO₃ and ZnO-NPs were achieved using a Thermo Scientific Nicolet 380 Spectrometer, USA, in the spectral range between 4000 cm⁻¹ and 600 cm⁻¹ with a

resolution of 4 cm⁻¹ and 32 scans. The samples were prepared by pressing 100 mg of KBr and 2 mg of powder to give a thin disk. A reference spectrum of a pure KBr disk is used.

2.3.3. Scanning electron microscopy (SEM)

The morphology of the nanomaterials was detected using a scanning electron microscopy (SEM) (High Resolution Quanta FEG 250-SEM, Czech Republic) to investigate the filler dispersion and the compatibility between polymer and filler. The surfaces of the samples were examined without coated gold and at low vacuum.

2.3.4. Transmission electron microscopy (TEM)

The structure and surface morphology of the prepared ZnO-NPs and its nanocomposites were studied using JEOL JEM-1230 transmission electron microscope (TEM) with acceleration voltage of about 80 kV. The nanocomposite samples were prepared by adding a small drop of the dispersion of polymer bio-nanocomposites onto a Lacey carbon film-coated copper grid and allowed to dry initially in air then by applying high vacuum

3. Results and discussion

In this paper, the authors offer a solution to one of the most significant challenges of the drilling fluids in HPHT (high pressure high temperature) wells circulation as (Table 2); carrying the drill cuttings back to the surface for continuous polymers has been widely used as drilling additives because of their unique structure that makes them able to plug pores, and stand the high temperature and pressure conditions. Conversely, the properties of the mud can be further enhanced by using nanomaterials that can enable the drilling fluid to function better under extreme conditions.

Electrical stability (ES) of an oil base mud is considered a measure of its emulsion stability. In the laboratory, a mud with a high degree of emulsion stability is generally smooth, shiny and does not adhere to the stirring spindle of a mixer. By contrast, a mud with a low degree of emulsion stability is dull, grainy and shows a marked tendency adhere to the spindle. The oil wetness or oil wetting tendency of an invert emulsion mud is defined here as the ability of the mud to incorporate foreign materials into the external, or oil phase. A mud with high emulsion stability is phase. A mud with high emulsion stability is oil wet, by definition, but may not necessarily be oil wetting.

3.1. Structure of ZnO nanoparticles

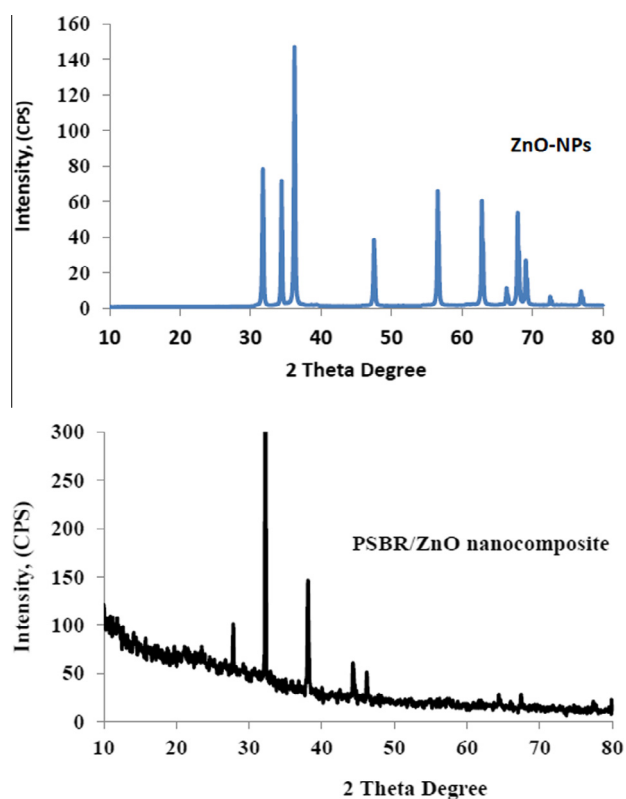
The XRD patterns of ZnO nanoparticles and PSB/ZnO nanocomposites are displayed in Fig. 1. The XRD profile ZnO-NPs showed characteristic peaks corresponding to the planes (100) at $2\theta = 30.74^\circ$, (002) at $2\theta = 34.5^\circ$, (101) at $2\theta = 36.8^\circ$, (102) at $2\theta = 47.7^\circ$, (110) at $2\theta = 56.2^\circ$, (103) at $2\theta = 61.7^\circ$ and (112) at $2\theta = 67.6^\circ$. This XRD pattern shows that the preparation of ZnO-NPs leads to wurtzite phase and all the diffraction peaks agree with the reported JCPDS data. This was confirmed by TEM observation, in which ZnO-NPs appear as spherical particles with size around 6 nm as shown in (Fig. 2). Furthermore, the XRD patterns of

Table 1 Composition of oil base mud.

Diesel	238 ml
Emulsifier	4.2 ml
Wetting agent	1.7 ml
Viscofire	8 g
Lime	3 g
Barite	255 g
Filter loss reducer	2.5 g
Fresh water	(33 ml water + 15 g CaCl ₂)

Table 2 Influence of polymer nanocomposites based on modified nano-CaCO₃ and ZnO-NPs on oil base mud.

Composition	Before hot rolling (temperature 120 °F, pressure 500 psi)				After hot rolling (temperature 300 °F, pressure 500 psi)				Before hot rolling/after Fluid loss (ml/30 min) (temperature 120 °F, pressure 500 psi)	Before hot rolling/after E. stability (beek volt) (temperature 300 °F, pressure 500 psi)
	RPM	Results	PV	Yield point	RPM	Results	PV	Yield point		
Blank (PSBR)	600	60	22	16	600	58	21	15	15/12	1200/850
	300	38			300	36				
	200	29			200	28				
	100	22			100	22				
	6	10			6	9				
	3	8			3	8				
0.5 modified nano-CaCO ₃ with 0.5 g. PSBR after 16 h	600	77	27	23	600	71	25	21	10/7	1200/1550
	300	38			300	36				
	200	29			200	28				
	100	22			100	22				
	6	10			6	9				
	3	8			3	8				
0.5 ZnO-NPs with 0.5 PSBR after 16 h	600	88	31	26	600	83	29	25	11/6	1220/1850
	300	57			300	54				
	200	43			200	40				
	100	34			100	33				
	6	14			6	13				
	3	12			3	12				

**Figure 1** XRD pattern of ZnO-NPs as well as PSBR/ZnO nanocomposite.

PSB/ZnO nanocomposite exhibited a broad, noncrystalline peak of polymer and more intense and crystalline diffraction peaks of ZnO-NPs. The occurrence of ZnO-NPs creates

neither new peak nor peak shifts with respect to PSB which indicates that ZnO-NPs filled embed into polymer matrix consists of two-phase structures.

3.1.1. Transmission electron microscopy (TEM)

Single crystalline ZnO nanoparticles were manufactured by a hydrothermal method; zinc acetate and 0.5 M NaOH were used to prepare ZnO-NPs at 150 °C for 6 h using absolute ethanol. TEM image confirms the formation of ZnO-NPs with an average size around 6 nm, which is in good agreement with XRD results (Fig. 2). The ZnO-NPs in the range of nanometer grade have a good dispersibility in PSBR matrix. The dark zones correspond to the crystalline ZnO-NPs although the bright zones point to the amorphous PSBR matrix, because of the high electron density of the ZnO-NPs.

3.1.2. Scanning electron microscopy (SEM)

SEM images were obtained using a voltage of 20 kV. The surfaces of the ZnO-NPs and PSBR/ZnO nanocomposite films were studied using SEM are shown in (Fig. 3) ZnO nanoparticles (average size, 6 nm) are found to be homogeneously dispersed in the PSBR matrix. The efficiency of nanoparticles in improving the properties of the polymer material is primarily determined by the degree of dispersion in the matrix. These nanostructured ZnO in the polymer can change the thermal and optical properties of the composite. The size of the ZnO nanoparticles in the PSBR matrix corresponds to that of primary particles, except for a very few agglomerates.

3.1.3. Infrared (IR) spectral analysis

In order to establish probable intermolecular interactions among components in the system, FT-IR spectroscopy measurements were carried out. Fig. 4 FT-IR spectra of ZnO-NPs, the bands observed at 424, 453, and 527 cm⁻¹ are

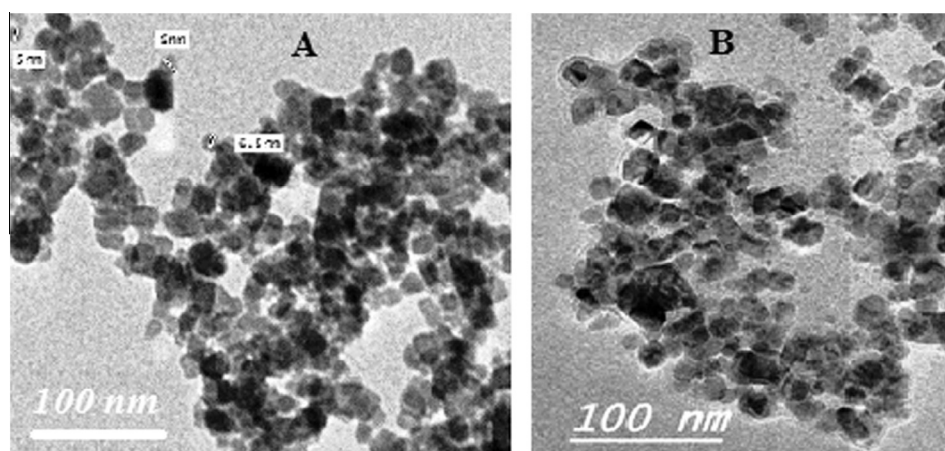


Figure 2 (A and B) TEM of ZnO-NPs prepared by hydrothermal method and PSBR/ZnO nanocomposite.

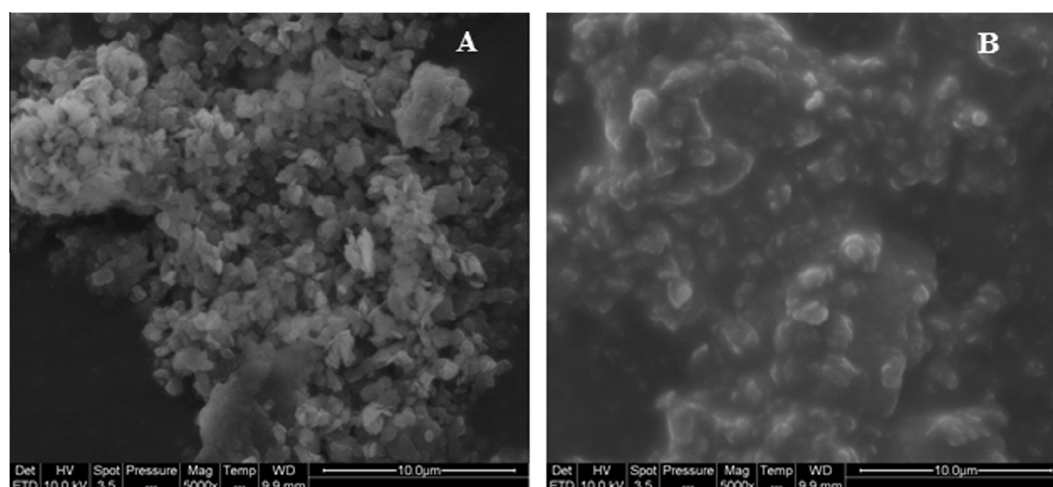


Figure 3 SEM images of (A) ZnO-NPs, (B) PSBR/ZnO nanocomposite.

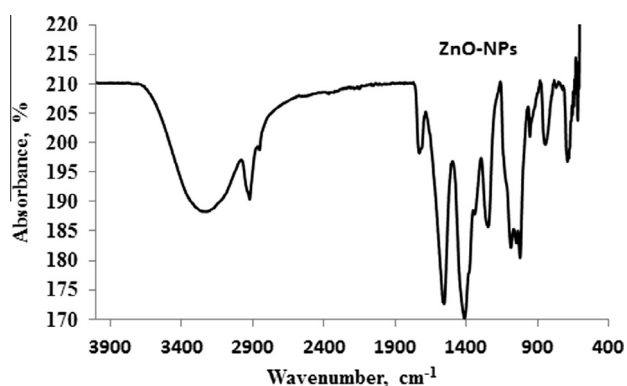


Figure 4 FT-IR spectra of ZnO-NPs.

assigned to Zn-O vibrations [18,19] out of which the bands at 453 and 527 cm^{-1} are present in the ZnO-NPs spectrum confirming the formation of ZnO-NPs. The three bands centered at 1338, 1412, and 1572 cm^{-1} detected in the ZnO-NPs spectrum are ascribed to the stretching vibrations of C=O, C=C, and C-H groups in acetate species. The favorable

intermolecular interactions between these groups and nanoparticles affected the variations in the characteristic absorption bands.

3.2. The surface morphology of modified CaCO_3 nanoparticles

3.2.1. X-ray diffraction patterns (XRD)

Fig. 5 displays the analysis of crystal structure using XRD for nano- CaCO_3 powders. The results established that the chief diffraction peaks of the crystalline structures of the nano- CaCO_3 are in the range 25°–55°. This indicates the presence of nano- CaCO_3 in crystalline and nanoform which revealed that the calcium carbonate is described by two characteristic crystal phases: aragonite and calcite.

3.2.2. Transmission electron microscopy (TEM) and SEM

The morphology structure and the dispersion of CaCO_3 nanoparticles were carried out using TEM and SEM. Fig. 6 (b) exhibited the TEM images of modified CaCO_3 nanoparticles using stearic acid. Also, Fig. 6(a) represented the SEM image of modified CaCO_3 nanoparticles using stearic acid. It is shown in Fig. 6(a) that some of the modified CaCO_3

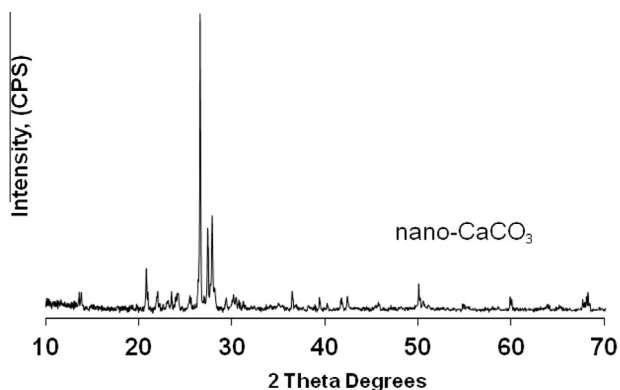


Figure 5 The XRD patterns of nano- CaCO_3 powder.

nanoparticles were seriously aggregated and lapped over and the particle size ranged from 64 to 100 nm. Also, it was shown from Fig. 6(b) that stearic acid modified nano- CaCO_3 was dispersed well and individual nanoparticles could be distinguished. These results confirmed that the phenomena of nanoparticles agglomeration decreased effectively because the nanoparticles were kept apart by the surface-modification layer of stearic acid and increased the activity of the modified CaCO_3 nanoparticles. A few studied the surface modification of CaCO_3 nanoparticles by stearic acid and the effect of

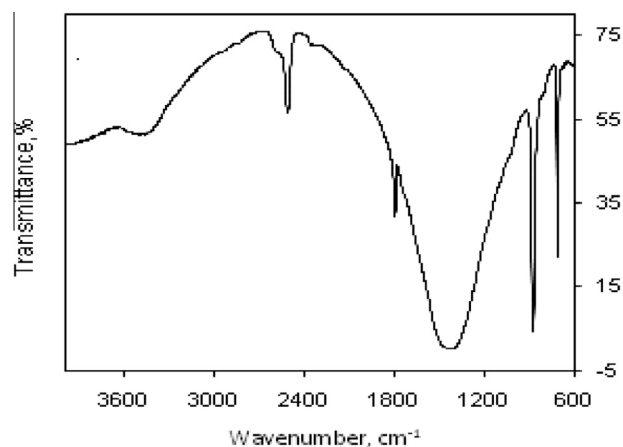


Figure 7 FT-IR spectrum of the CaCO_3 nanoparticles.

modified- CaCO_3 nanoparticles cannot be stably dispersed in non-polar organic solvents.

3.2.3. Infrared (IR) spectral analysis

From the FTIR spectrum of CaCO_3 nanoparticles illustrated in Fig. 7, it can be seen that the CaCO_3 nanoparticles had adsorption bands at $2950\text{--}2840\text{ cm}^{-1}$, corresponding to the vibration mode of C-H of stearic acid, and also 707, 873

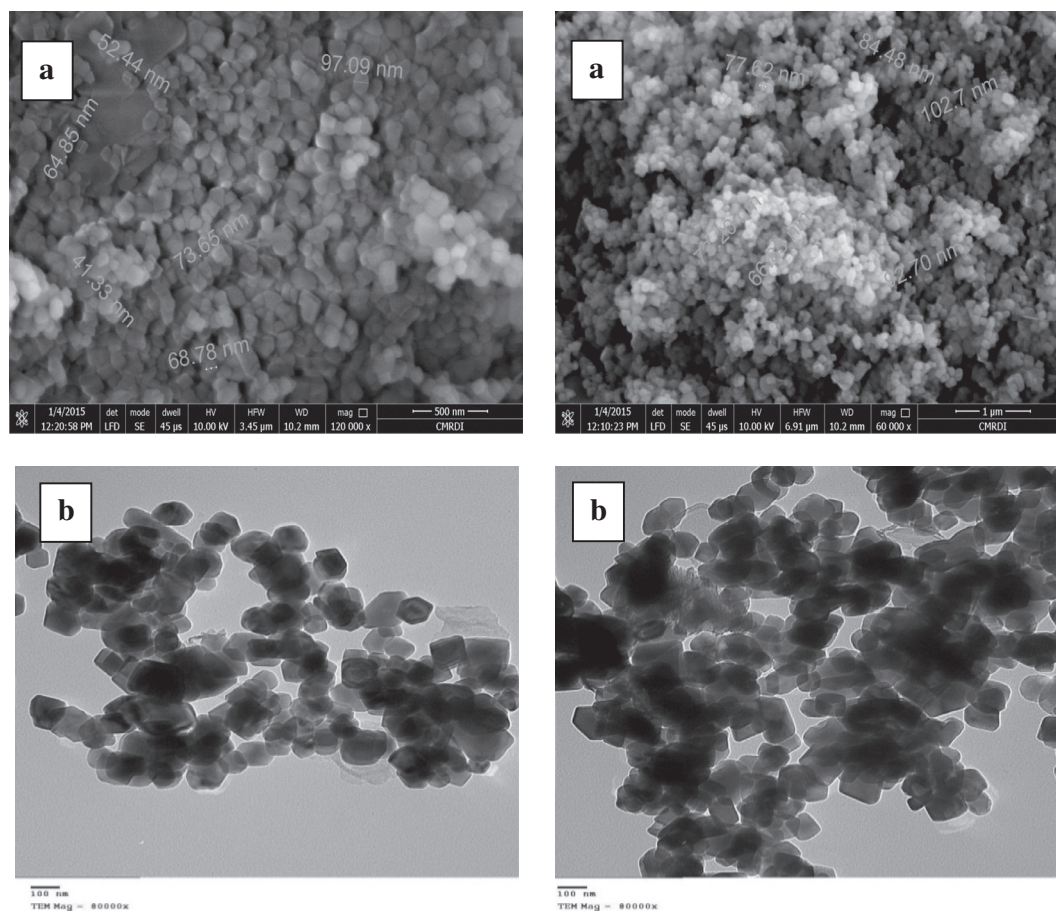


Figure 6 SEM image of modified nano- CaCO_3 (a) as well as TEM image (b) with different magnifications.

and 1418 cm^{-1} corresponding to the in-, out-plane bending and asymmetrical stretching vibration peaks of $\text{O}-\text{C}-\text{O}$, respectively. They all are characteristic peaks in calcite [20,21].

3.3. Influence of PSBR nanocomposites on properties of mud rheology

From Table 2 when adding 0.5 of modified calcium carbonate with 0.5 of the PSBR polymer on oil base mud, it was observed that the yield point increased from 16 to 23, and the fluid losses decreased from 12 to 7 while the electrical stability increased from 850 to 1550. Also, the addition 0.5 of ZnO-NPs to 0.5 PSBR polymers, significant increases are observed in both the plastic viscosity from 22 to 31 and yield point from 16 to 26, whereas the fluid losses decreased from 12 to 6 and the electrical stability increased from 850 to 1850 beek volt. From this result we can conclude that the using of polymer nanocomposites based on ZnO-NPs enhanced the yield point at high pressure high temperature wells more than polymer nanocomposites based on modified nano- CaCO_3 .

3.4. Effect of viscosity (yield point) on cutting recovery, fluid losses and electrical stability on mud rheology

The viscosity of oil base mud increases as the amount of polymer nanocomposites containing zinc oxide nanoparticles and modified calcium carbonate nanocomposites increase. Table 2 shows the effect of adding polymer nanocomposites loading with ZnO-NPs and modified nano- CaCO_3 to oil base mud exciting capacity for various flow rates. The percentage of the cutting recovery displays the mud ability to lift cuttings from the bottom hole to the surface. Fluid losses decreased as the nanocomposites containing ZnO-NPs and modified nano- CaCO_3 added to the oil base mud to solve many hole problems as sloughing in shaly formation. These changes depend on the cutting size and annular velocity. The enhancement of cutting recovery is very significant for small cutting size as compared to the bigger cutting size. Moreover, the improvement in mud cutting lifting capacity is owing to addition of 0.5 nanoparticles with 0.5 polymers to the mud, since the nanocomposite product will improve the mud rheological properties. The nanoparticle material can enhance the stability against oil base mud subsequently the surface forces can easily balance the gravity force. When the force acts downward, it has less potential to settle down to the bottom of borehole. Consequently, under these conditions, the cutting scan is easily transported to the surface. But, this is not always true because the high viscosity can be achieved when the dispersion of clays in the mud is high. From this study, adding PSBR nanocomposites based on ZnO-NPs and modified nano- CaCO_3 to oil base mud will influence mud viscosity, gel strength and fluid losses.

When adding 0.5 g of PSBR nanocomposites to the mud sample, the electrical stability value rises from 850 to 1550 and 1850; this means that the charge of mud in liquid phase is equal to solid phase, which leads to the stability of mud at high pressure high temperate wells and improves the yield point and fluid losses.

In general, high gel strength of mud increases the viscosity. Nonetheless, this is not always true because the high viscosity can be accomplished when the dispersion of clays in the mud is

excessive. From this study, adding zinc oxide nanoparticles and modified calcium carbonate nanoparticles to the oil base mud will influence yield point, gel strengths, fluid losses and electrical stability, and these unique nanoparticles can be utilized as fluid viscosity stabilizer to significantly improve the cutting recovery.

4. Conclusion

The present work has revealed that the preparation of ZnO-NPs by a hydrothermal method and modification of nano- CaCO_3 then using the prepared nanoparticles to manufactured polymer(PSBR) nanocomposites based on nano- CaCO_3 and ZnO-NPs successfully fabricated by a melt intercalation method. The prepared nanomaterials and polymer nanocomposites were characterized via XRD, SEM, IR and TEM. The SEM micrographs displayed that the nanocomposite becomes more homogeneous than the former polymer matrix. Also, TEM micrographs show good dispersion of nanoparticles within polymer matrix when using ZnO-NPs as filler. Correspondingly, the prepared polymer nanocomposites were used for high pressure high temperature (HPHT) drilling of oil base mud on diverse loading of ZnO-NPs and nano- CaCO_3 , and the rheological properties of oil base mud were evaluated and enhanced the yield point at high pressure high temperature wells (HPHT). The achieved results are very encouraging and also the using of polymer nanocomposites is sensible for the increase of apparent viscosity, plastic viscosity and yield point at high temperature. Consistently, the prepared nanocomposites demonstrated increase of apparent viscosity, plastic viscosity, and yield point, decrease in fluid loss and increase in electrical stability at high pressure high temperature wells. From all the obtained results, ZnO-NPs and modified nano- CaCO_3 as well as polymer nanocomposites are novel materials that can be used for high pressure high temperature wells (HPHT) owing to the improvement of yield point, increasing electrical stability and declining fluid losses.

References

- [1] N. Danvers, *Fluid Mechanics*, Addison-Wesley Publishing Company, 1977.
- [2] *Standard Procedure for Testing Drilling Fluids*, API RP 13B-1, second ed., American Petroleum Institute, Dallas, September 1997.
- [3] W.E. Rogers, third ed., *Composition and Properties of Oil Well Drilling Fluids*, vol. 19, Gulf Publishing Co., Houston, 1963, p. 395.
- [4] J.P. Plank, *Oil Gas J.* 90 (1992) 40–45.
- [5] R.K. Clark, R.F. Scheurman, H. Rath, H.G. Van Laar, *J. Petrol. Technol.* 28 (1976), 6426.5 I.
- [6] A. Usuki, Y. Kojima, M. Kawasumi, A. Okada, Y. Fukushima, T. Kurauchi, O. Kamigaito, *J. Mater. Res.* 8 (1993) 1179–1184.
- [7] T. Lan, T. Pinnavaia, *Chem. Mater.* 6 (1994) 2216–2219.
- [8] P.M. Ajayan, L.S. Schadler, P.V. Braun (Eds.), *Nanocomposite Science and Technology*, Wiley VCH, Weinheim, 2003.
- [9] A.M. Youssef, *RSC Adv.* 4 (2014) 6811–6820.
- [10] A.M. Youssef, M.S. Abdel-Aziz, *Polym. Plast. Technol. Eng.* 52 (2013) 607–613.
- [11] V. Fombuena, L. Bernardi, O. Fenollar, T. Boronat, R. Balart, *Mater. Des.* 57 (2014) 168–174.
- [12] R. Doufnoune, F. Chebira, N. Haddaoui, *Int. J. Polym. Mater.* 52 (2003) 967–984.

- [13] Z.L. Wang, *J. Phys.: Condens. Matter* 16 (2004) R829–R858.
- [14] C. Riggio, V. Raffa, A. Cuschieri, Synthesis, characterisation and dispersion of zinc oxide nanorods for biomedical applications, *Micro Nano Lett.* 5 (2010) 355–360.
- [15] Y. Liu, T. Morishima, T. Yatsui, T. Kawazoe, M. Ohtsu, *Nanotechnology* 22 (2011) 215605 (5 pp).
- [16] A.M. Youssef, H. Abou-Yousef, S.M. El-Sayed, S. Kamel, *Int. J. Biol. Macromol.* 76 (2015) 25–32.
- [17] A.M. Youssef, T. Bujdosó, V. Hornok, S. Papp, B. Kiss, A. Abd El-Hakim, I. Dékány, *Appl. Clay Sci.* 77–78 (2013) 46–51.
- [18] J.J. Schneider, R.C. Hoffmann, J. Engstler, A. Klyszcz, E. Erdem, P. Jakes, R.A. Eichel, L. Pitta-Bauermann, J. Bill, *Chem. Mater.* 22 (2010) 2203–2212.
- [19] S.A. Vorobyova, A.I. Lesnikovich, V.V. Mushinski, *Mater. Lett.* 58 (2004) 863–866.
- [20] J.K. Yong, H.K. Kyoung, S.L. Chang, B.S. Kwang, *J. Ceram. Process. Res.* 3 (2002) 146–149.
- [21] R. Siddheswaran, R. Sankar, M. Ramesh Babu, M. Rathnakumari, R. Jayavel, P. Murugakoothan, P. Sureshkumar, *Cryst. Res. Technol.* 41 (2006) 446–449.